

Article

# Insights into the Fouling Propensities of Natural Derived Alginate Blocks during the Microfiltration Process

Shujuan Meng <sup>1</sup>, Rui Wang <sup>1</sup>, Minmin Zhang <sup>2</sup>, Xianghao Meng <sup>1</sup>, Hongju Liu <sup>1</sup> and Liang Wang <sup>3,\*</sup>

<sup>1</sup> School of Space and Environment, Beihang University, Beijing 100191, China; mengsj@buaa.edu.cn (S.M.); rui\_wang@buaa.edu.cn (R.W.); SY1930212@buaa.edu.cn (X.M.); liuhj@buaa.edu.cn (H.L.)

<sup>2</sup> Chemical Engineering, Xiamen University, Xiamen 361005, China; mmzhang666@gmail.com

<sup>3</sup> State Key Laboratory of Separation Membranes and Membrane Processes, Tiangong University, Tianjin 300387, China

\* Correspondence: mashi7822@163.com; Tel.: +86-186-026-50716

Received: 15 October 2019; Accepted: 14 November 2019; Published: 17 November 2019



**Abstract:** Membrane technology has been one of the most promising techniques to solve the water problem in future. Unfortunately, it suffers from the fouling problem which is ubiquitous in membrane systems. The origin of the bewilderments of the fouling problem lies in the lack of deep understanding. Recent studies have pointed out that the molecular structure of foulant affects its fouling propensity which has been ignored in the past. In this study, the filtration behaviors of alginate blocks derived from the same source were comprehensively explored. Alginate blocks share the same chemical composition but differ from each other in molecular structure. The alginate was first extracted from natural seaweed using calcium precipitation and ion-exchange methods. Extracted alginate was further fractionized into MG-, MM- and GG-blocks and the characteristics of the three blocks were examined by Fourier transform infrared spectroscopy (FTIR) and field emission scanning electron microscopy (FESEM) observations, and transparent exopolymer particles' (TEPs) measurements. Results showed that MG-, MM- and GG-blocks had the same functional groups, but they showed different intermolecular interactions. TEP formation from MG-, MM- and GG-blocks revealed that the molecule crosslinking of them decreased in the order of MM-blocks > GG-blocks > MG-blocks. It was further found from microfiltration tests that these alginate blocks had completely different fouling propensities which can be explained by the TEP formation. TEPs would accumulate on membrane surfaces and worked as a pre-filter to avoid serious pore blocking of membrane. That all suggested that the membrane fouling was closely related to the molecular structure of foulant. It is expected that this study can provide useful insights into the fouling propensities of different types of polysaccharides during filtration processes.

**Keywords:** membrane fouling; molecular composition of foulant; transparent exopolymer particles (TEP); fouling propensities

## 1. Introduction

Water scarcity is one of the most serious crises in the world as a result of the uneven distribution of water resources, poor water management and climate change. To cope with this situation, scientists and engineers have been working hard to develop treatment methods of every sort [1–4]. Most of the efforts aim to remove the pollutants in water bodies and to increase water supplies via the reliable reuse of wastewater and efficient desalination of seawater and brackish water [5,6]. In the past few decades, membrane technology has been widely used around the world as a promising

technique for water treatment [7–9]. However, membrane fouling still remains one of the obstacles to the successful operation of membrane systems, as it has since the day that membrane filtration was employed [10]. Among all fouling problems, organic fouling has often been reported to be a major type and polysaccharides play a key role in organic fouling. Compared to other organic foulants, such as proteins and humic acid, the chains of polysaccharides are usually much longer and prone to gelling to form gel layer on a membrane surface via interaction of the molecular chain. However, the exact fouling propensities of polysaccharides are not clear, especially the influence of molecular structure on fouling. As a consequence of this, more efforts should be devoted to the investigation of the filtration behaviors of polysaccharides, relating the information of molecular structure with fouling tendencies.

Recently, it has been found that polysaccharides can aggregate together to form three-dimensional networks; i.e., transparent exopolymer particles (TEPs). The role of TEPs in membrane fouling has attracted more and more attention since Berman and Hølenberg first pointed out that they may participate in the fouling problems in membrane systems [11]. TEPs are planktonic hydrogels in water environments which are mainly formed by polysaccharides via an abiotic pathway [12]. TEPs possess a high viscosity; thus, they can attach to the membrane surface easily to develop a gel layer [13]. More importantly, it is difficult to remove TEPs from a membrane system. TEPs are deformable; thus, they also can penetrate into membrane pores whose sizes actually are smaller than the dimensions of TEP under pressure. In addition, some of TEPs will break into small pieces at the feed side and then reassemble into larger forms at the filtrate side of membrane at the aid of stream turbulence and divalent cations [14]. Thus, TEPs are dynamic in membrane systems, which poses difficulties in identifying the exact nature of TEP fouling. The effect of TEPs on membrane fouling needs to be further explored.

Alginate is a typical model polysaccharide that is commonly employed in studies of membrane fouling. Alginate is unbranched binary copolymer consisting of  $\beta$ -D-mannopyranuronic acid (M) and  $\alpha$ -L-gulopyranuronic acid (G) which combines into MG-, MM- and GG-blocks in varying proportions [15]. These blocks play different roles in alginate chains; i.e., GG-blocks are responsible for the gel-forming capacity, and MG- and MM-blocks provide flexibility to the chains [16]. Their proportions, distributions and lengths determine the chemical and physical properties of alginate molecules. So far, there are more than 200 kinds of alginates derived from different sources [17] which are different in MG-, MM- and GG-blocks contents [18]. It is reasonable to consider that alginates extracted from different algal sources may behave differently during membrane filtration processes. Since alginate has been commonly used as a model organic foulant in numerous studies of membrane fouling, a new challenge on the interpretation and reliability of filtration data would appear if alginate used in filtration experiments was not well characterized. Therefore, in this study, alginate was directly prepared from dry seaweed using alkaline extraction and then block fractionation was performed. Subsequently, three kinds of alginate blocks were systematically characterized with Fourier transform infrared spectroscopy (FTIR) and field emission scanning electron microscopy (FESEM). Dead-end filtration tests were employed to examine the fouling propensities of MG-, MM- and GG-blocks under the same experimental conditions. In addition, TEP measurement was also performed to evaluate the influence of TEP on membrane filtration.

## 2. Materials and Methods

### 2.1. Alginate Extraction from Raw Seaweed

Alginate used in this study was extracted from Fuerji dried seaweed according to the following steps. Seaweed was chopped into small pieces and 5 g of chopped dry seaweed was soaked in 300 mL of 1% formaldehyde (Sigma, City of Saint Louis, MO, USA) for 4 h. After that, seaweed pieces were washed by deionized water (Milli-Q, Burlington, MA, USA) to remove excess formaldehyde residue. Subsequently, rinsed seaweed was soaked in 300 mL of 3% Na<sub>2</sub>CO<sub>3</sub> (Merck, Kenilworth, NJ, USA) solution for 3 h, and alginate was converted to a soluble form so that it could be separated from the

insoluble seaweed residue. After alkaline soaking, the solution became very sticky and a clean cloth was used first to remove the bulk seaweed residue, and that was followed by filtration using filter papers. After careful addition of 50 mL of 10%  $\text{CaCl}_2$  (Merck, Kenilworth, NJ, USA) into the above alginate solution, woolly cloudlike aggregates formed. The aggregates were quickly transferred to a clean beaker. Ion exchange was employed to convert calcium alginate to sodium alginate. A series of ion exchanges, 20 min each, were carried out to get rid of the  $\text{Ca}^{2+}$  until no white precipitate formed when  $\text{Na}_2\text{CO}_3$  was added into the exchanged solution. Finally, an equal volume of ethanol (Merck, Kenilworth, NJ, USA) was added to precipitate sodium alginate.

## 2.2. Block Fractionation of Alginate

The extracted alginate was fractionated according to the method proposed by Leal et al. as presented in Figure 1 [19]. Firstly, 10 g/L alginate was prepared with Millipore water. The solution was stirred for 2 h for complete dissolution. Then, HCl (Merck, Kenilworth, NJ, USA) was slowly added into the sodium alginate solution with stirring, forming white cloudlike aggregations. The solid-liquid mixture was subsequently heated at 100 °C in an oil bath for 0.5 h. After heating, the cloudlike aggregations were partially dissolved and the mixture was centrifuged at 10,000 rpm for 30 min. The supernatant solution was neutralized with 1 M NaOH (Merck, Kenilworth, NJ, USA) and precipitated with an equal volume of ethanol. The white precipitation was separated by another 30 min of centrifugation at 10,000 rpm and freeze-dried (MG-blocks). The insoluble residue from the first centrifugation was re-dissolved in 1 M NaOH and the pH was readjusted to 2.85 by adding 1 M HCl. At pH 2.85, new precipitation developed and centrifugation was used for separation. The soluble fraction was again neutralized with 1 M NaOH, precipitated by ethanol and freeze-dried (MM-blocks). The solid fraction was re-dissolved in 1 M NaOH, neutralized by 1 M HCl, precipitated by ethanol and freeze-dried (GG-blocks).

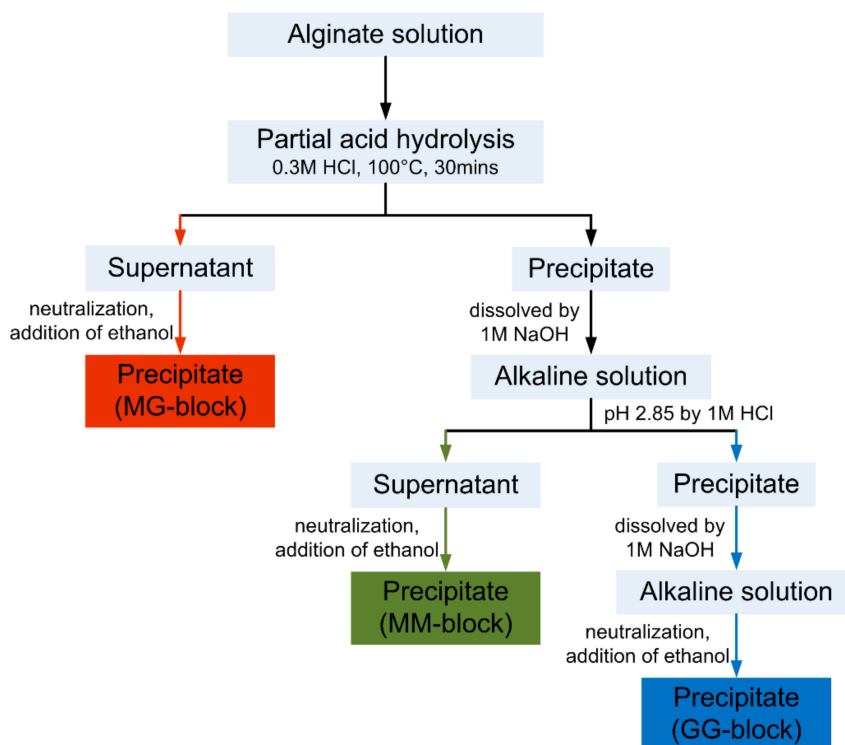


**Figure 1.** The alginate fractionation procedure employed to obtain MG-, MM- and GG-blocks.

### 2.3. FTIR Spectroscopy of Alginate Blocks

In order to characterize the alginate blocks, the FTIR spectra of the MG-, MM- and GG-blocks fractionated from the extracted alginate were measured. The alginate blocks obtained from commercial alginate sodium (Wako, Tokyo, Japan) via the same procedure were also measured by FTIR to provide a direct comparison. Sample preparation was done by the FTIR Start Kit and 300 mg of KBr (Merck, Kenilworth, NJ, USA) was used to create the baseline. An amount of 2–4 mg of sample was mixed with 295 mg KBr and ground for a short time in order to mix it thoroughly. Then, the pure KBr disc and alginate-KBr mixture pellets were transferred to the disc holder which was subsequently inserted into the spectrometer. The FTIR spectra were recorded using a PerkinElmer FTIR Spectrum GX 50905 (PerkinElmer, Waltham, MA, USA). A total of 60 scans were taken for both background establishment and sample measurements.

### 2.4. Field Emission Scanning Electron Microscope (FESEM) Observations

In order to visualize the micro-structures of the alginate, MG-, MM- and GG-blocks we prepared, the powders of them were completely freeze-dried and they were examined by an FESEM (Jeol JSM-7600F, Tokyo, Japan). These powder samples were coated with Pt just before observation to increase electrical conductivity. Besides, the TEPs formed from alginate blocks were also observed by the FESEM. Solutions of MG-, MM- and GG-blocks were gently filtered by the 0.05  $\mu\text{m}$  filters under a pressure below 0.2 bars and then freeze-dried to keep the morphology of TEP. Subsequently, these samples were observed and at least 10 pictures for each sample were recorded. In addition, the fouled membrane pieces were also examined by the FESEM to provide a direct observation of the fouling development of the membrane. Membrane samples were taken from the same location from the fouled membrane and representative images were taken.

### 2.5. TEP Determination

TEP measurements were carried out for the MG-, MM- and GG-blocks samples. The determination procedure was the same as in our previous study [20,21]. Alcian blue was used to stain the TEP sample and preparation involved dissolving alcian blue 8 GX (0.02%) (Sigma, City of Saint Louis, MO, USA) into 0.06% acetic acid before the tests. To quantify the TEP formed from different alginate block samples, solutions of MG-, MM- and GG-blocks were prepared. The alginate blocks had smaller sizes than a whole molecule chain of alginate; thus, filters with smaller sizes were used to determine the TEP. To look into the detailed size distributions of TEPs formed from alginate blocks, 0.2  $\mu\text{m}$  and 0.05  $\mu\text{m}$  polycarbonate filters (Whatman, Maidstone, UK) were used to conduct the TEP tests. Alginate block solutions were filtered through 0.2  $\mu\text{m}$  and 0.05  $\mu\text{m}$  filters at a constant vacuum of 0.2 bars. The retained TEP on filter was stained by alcian blue solution and subsequently rinsed with 1 mL of Milli-Q water after ~5 s staining. The filter together with stained TEPs were immersed in a beaker with 5 mL of 80%  $\text{H}_2\text{SO}_4$  solution for 2 h, and we made sure all alcian blue was dissolved into the sulfuric solution. Finally, the absorbance of sulfuric acid solution was measured with a UV-Vis spectrophotometer (Shimadzu, Kyoto, Japan) at 787 nm wavelength and TEP concentration was expressed as mg gum xanthan equivalent per liter of water ( $\text{mg X}_{\text{eq}}\cdot\text{L}^{-1}$ ).

### 2.6. Dead-End Filtration Tests

Standard dead-end filtration, as shown in Figure 2, using nylon membrane with a pore size of 0.2  $\mu\text{m}$ , was chosen to examine the different fouling potentials of the MG-, MM- and GG-blocks. The effective membrane surface area was 11.94  $\text{cm}^2$ , and the filtration process was driven by compressed nitrogen gas at 1 bar. The mass of the filtrate was recorded at the time interval of 10 s by an electronic balance with data-logging system installed in the connected computer. Feed solution was prepared with 0.01 M NaCl and 0.05 g/L alginate samples of respective blocks. A 20 min long initializing period with 0.01 M NaCl was conducted to make sure that stable performance of the membrane was

achieved. Subsequently, the samples of alginate blocks were filtered and the mass change of the filtrate was recorded.

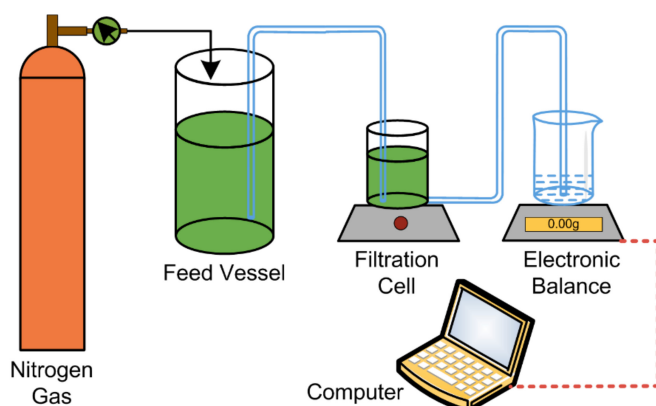


**Figure 2.** Schematic diagram of the dead-end filtration system used in this study.

### 3. Results and Discussion

#### 3.1. Block Composition of Alginate

Extracted alginate from the seaweed was fractionated using partial acid hydrolysis. The results showed (Table 1) that 19.2% MG-blocks, 62.4% MM-blocks and 19.3% GG-blocks made up the alginate chains, suggesting that MM-block is the main component of the sodium alginate we extracted. The commercial alginate (Sigma, City of Saint Louis, MO, USA) contained 13.8% MG-blocks, 53.5% MM-blocks and 32.7% GG-blocks, which also indicated that the main component in alginate was MM-blocks. These results were consistent with the literature reports that for most alginates MM-blocks dominated molecular composition [15]. According to the above result, the M/G ratios in the extracted alginate could be calculated to be 2.51, which was consistent with the literature in which M/G ratio was within the range of 0.33–9 [15]. It should be noted that different seaweed species could yield different M/G ratios, even the same species from different seasonal and growth conditions. For example, the M/G values of alginates from *Lessonia vadosa* blades collected at the same locality in winter and spring varied between 0.79 and 0.33 [22]. Therefore, it is of primary importance to pay attention to the chemical composition of the polysaccharide that was subjected to filtration. The alginate used in this study was extracted from the natural seaweed. It provided a different and more natural source for alginate blocks compared to the commercial alginate. In natural water environments, most of the TEPs form from the precursor materials (most of them are polysaccharides) secreted by algae via an abiotic pathway. Therefore, the alginate directly extracted from seaweed would be a good model for the TEP formation and polysaccharide fouling study.

**Table 1.** Molecular composition of extracted and commercial alginate.

	MG	MM	GG
Extracted alginate from the seaweed	19.2 ± 2.1%	62.4 ± 3.5%	19.3 ± 0.9%
Commercial alginate	13.8 ± 1.9%	53.5 ± 1.3%	32.7 ± 0.6%

#### 3.2. FTIR Spectrums of MG-, MM- and GG-Blocks

Figure 3 shows the respective FTIR spectrums of the MG-, MM- and GG-blocks derived from the seaweed and the commercial alginate. It can be seen that the alginate blocks showed similar absorption peaks to those obtained from commercial alginate. This observation suggested that the alginate we extracted had the same material composition with the commercial one, although all the alginate blocks had more impure peaks than commercial ones. The broad bands centered at wave

numbers of  $3393\text{ cm}^{-1}$ ,  $3401\text{ cm}^{-1}$  and  $3381\text{ cm}^{-1}$  were assigned to hydrogen bonded O–H stretching vibrations. The weak signals at wavenumbers of  $2923\text{ cm}^{-1}$ ,  $2935\text{ cm}^{-1}$  and  $2939\text{ cm}^{-1}$  were due to C–H stretching vibrations and the asymmetric stretching of carboxylate O–C–O vibration contributed to the strong absorptions at  $1618\text{ cm}^{-1}$ ,  $1610\text{ cm}^{-1}$  and  $1615\text{ cm}^{-1}$ . According to literature [19,23–25], the band at  $1420/1412/1419\text{ cm}^{-1}$  was assigned to C–OH deformation vibration with contribution of O–C–O symmetric stretching vibration of carboxylate group. The medium absorption at  $1305\text{ cm}^{-1}$ ,  $1303\text{ cm}^{-1}$  and  $1320\text{ cm}^{-1}$  in the three figures, respectively, may be assigned to O–C stretching vibration of carboxylic acid and derivatives [23]. In addition, the medium to strong IR absorption bands at  $1200\text{--}970\text{ cm}^{-1}$  are mainly due to C–C and C–O stretching in the pyranoid ring and C–O–C stretching of glycosidic bonds [25]. An intense absorption in this spectral region is common for all polysaccharides [26,27]. The fingerprint or anomeric region at  $950\text{--}750\text{ cm}^{-1}$  showed three characteristic absorption bands in all polysaccharide standards and alginate polysaccharides. The band at  $957/938/949\text{ cm}^{-1}$  was assigned to the C–O stretching vibration of uronic acid residues. The one at  $886/889/904\text{ cm}^{-1}$  was assigned to the C1–H deformation vibration of  $\beta$ -mannuronic acid residues. Finally, the band at  $814/820/812\text{ cm}^{-1}$  is characteristic of mannuronic acid residues [22]. Consequently, alginate was the main polysaccharide extracted from seaweed and the three blocks had the same functional groups as the commercial ones.

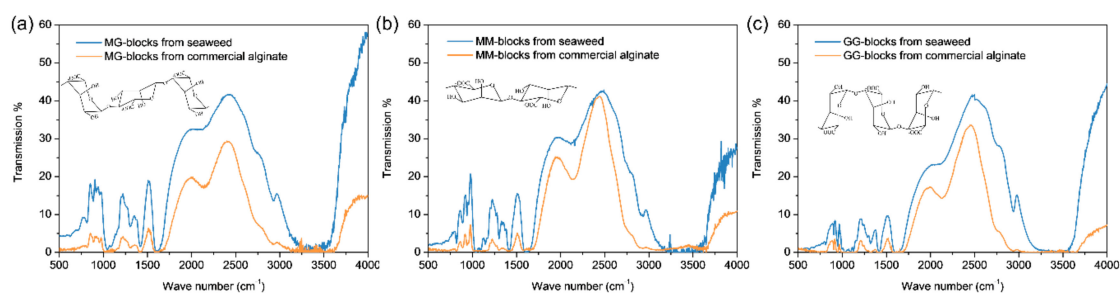


**Figure 3.** FTIR spectrum of alginate blocks derived from seaweed, and the commercial ones. (a) MG-blocks; (b) MM-blocks; (c) GG-blocks

### 3.3. The Micro-Structures of the Alginate, MG-, MM- and GG-Blocks

The dry powders of the alginate extracted from seaweed and the MG-, MM- and GG-blocks fractionated from the alginate were observed under an FESEM. As can be seen in Figure 4, the micro-structures of alginate and alginate blocks shared some similarities and discrepancies. All of the samples showed particle like structures (Figure 4a–d) but the detailed structures were different from each other (Figure 4e–h). These observations indicated that MG-, MM- and GG-blocks would have different chemical and physical properties which should have significant effects on their filtration behaviors.

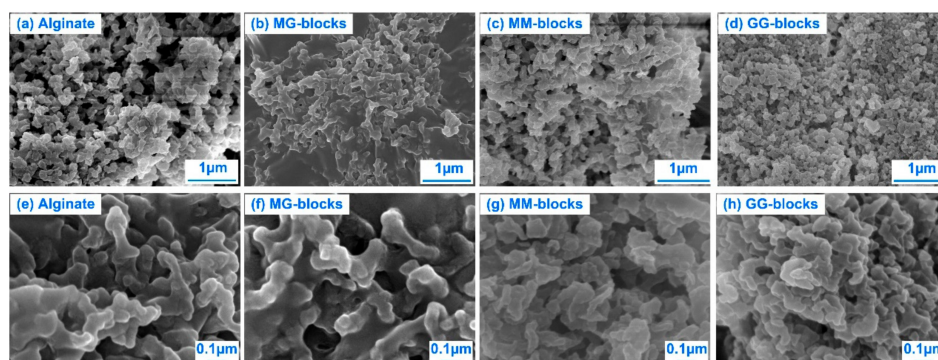


**Figure 4.** The micro-structures of the alginate, MG-, MM- and GG-blocks derived from the natural seaweed. (a) Alginate; (b) MG-blocks; (c) MM-blocks; (d) GG-blocks; (e)–(h) were the amplificatory observations of (a)–(d).

### 3.4. The TEP Formation from MG-, MM- and GG-Blocks

The TEP level formed from the 50 mg/L alginate blocks was measured to quantitatively assess their aggregation ability. To look into the size distribution of the TEP formed from MG-, MM- and GG-blocks, two sizes of filters were employed to conduct the measurements. As observed in Figure 5a, the highest TEP level was recorded in the MM-blocks determined with a 0.05  $\mu\text{m}$  filter, achieving 13.6 mg  $X_{\text{eq}}/\text{L}$  from the 50 mg/L alginate blocks. The MG- and GG-blocks produced 1.1 and 7.8 mg  $X_{\text{eq}}/\text{L}$  TEP respectively. This finding revealed that in the water environments, the polysaccharide chains would aggregate through molecule crosslinking instead of existing as single chains even at a low concentration. The TEP they formed via molecule crosslinking was much larger than their molecule size. From the TEP results, it could be found that the extent of molecule crosslinking decreased in the order of MM-blocks > GG-blocks > MG-blocks, which is consistent with the literature [28]. As shown in Figure 5, the highest TEP concentration was observed in the solution of MM-blocks, which was also the main component of alginate, as determined in the alginate fractionation. It revealed that although fractionated from the same alginate source, the MG-, MM- and GG-blocks possessed different abilities in molecular crosslinking due to their discrepancies in chain characteristics [28]. In addition, the TEP detected with a size larger than 0.2  $\mu\text{m}$  was remarkably smaller than the TEP formed with size bigger than 0.05  $\mu\text{m}$ , as shown in Figure 5b. That suggested that the TEPs formed from all alginate blocks were small in size and most of the TEPs had sizes ranging from 0.05  $\mu\text{m}$  to 0.2  $\mu\text{m}$ .

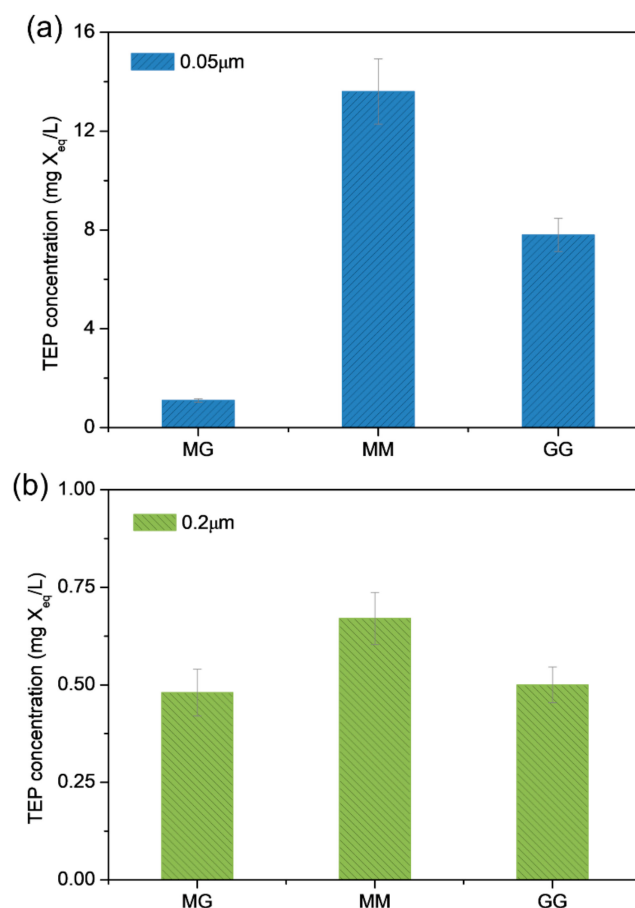


**Figure 5.** The TEP formation from MG-, MM- and GG-blocks. (a) TEP measured using 0.05  $\mu\text{m}$  filter and (b) TEP measured with 0.2  $\mu\text{m}$  filter.

Besides, the TEPs formed from alginate blocks were gently retained on the 0.05  $\mu\text{m}$  filters to provide a direct observation. As shown in Figure 6, the TEPs seemed like the result of crosslinked alginate blocks and had dimensions larger than a single molecule. TEPs actually were the aggregations

of alginate blocks. The formation of TEPs from these alginate blocks would definitely affect their filtration behaviors in membrane filtration process. The intermolecular interactions of foulants was essential in understanding fouling mechanism [29,30] and more efforts should be devoted into exploring the complex crosslinking of various foulants in water environments.

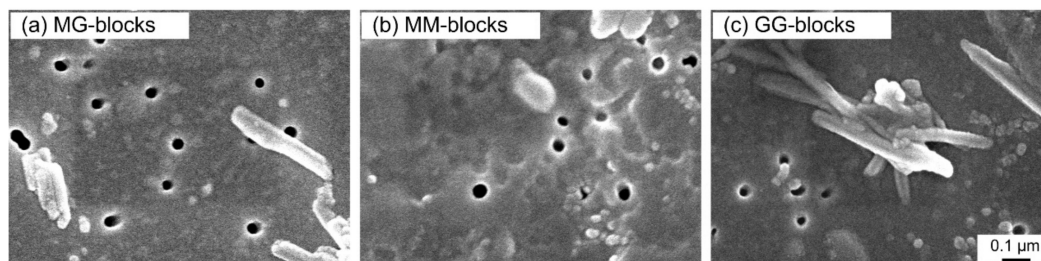


**Figure 6.** The observation of TEPs formed from (a) MG-, (b) MM- and (c) GG-blocks with FESEM (0.05  $\mu\text{m}$  filters).

### 3.5. Filtration Behaviors of MG-, MM- and GG-Blocks

Although the monomers M and G are isomers, MG-, MM- and GG-blocks displayed completely different filtration behaviors. As shown in Figure 7, the severest fouling happened in filtration of MG-blocks, and the least flux decline was observed during the filtration of MM-blocks. GG-blocks showed a fouling tendency between those of MG-blocks and MM-blocks. All these results suggest that differences lying in the molecular structures of these blocks lead to their diverse filtration properties. Combined with the TEP determination results, it can be deduced that the more TEPs formed, the less fouling that occurred during membrane filtration. TEPs possessed large sizes and easily attached on a membrane surface to form a fouling layer, which in turn prevented the serious pore clogging of membrane [28]. Thus, the least membrane fouling was recorded in the filtration of MM-blocks which showed the largest TEPs. On the contrary, the MG-blocks, which possessed the smallest size, would penetrate into the membrane pores and be absorbed onto the membrane pore walls resulting with the reduced radius and number of the effective membrane pores. The fouling propensities of alginate blocks derived from the commercial alginate decreased at the same order: MG-blocks > GG-blocks > MM-blocks, as can be seen in Figure 7b,c. These results were further evident from the FESEM observations of the fouled membrane surfaces as can be seen in Figure 8. After filtration with MM-blocks, some of a fouling layer can be observed on the membrane surface while there was very little fouling layer development on membrane surfaces after they were filtered by MG- and GG-blocks. Instead, the membrane pores seemed to be filled by foulants (Figure 8b,d). As a consequence of these results, it was found that the more TEP formed, the less serious a fouling problem was observed in the filtration process in this study. In this study, it was found that the TEP may work as a pre-filter to reduce the amount of alginate blocks that penetrated into membrane pores; thus, mitigating the membrane fouling. The TEP themselves certainly did not lead to serious membrane fouling. It depended on the sizes of membrane pores. Figure 6 showed the TEPs gently retained by 0.05  $\mu\text{m}$  filters and then freeze-dried to keep the morphology of TEPs. It could be seen that TEPs formed from the aggregation of alginate blocks and had bigger sizes than single molecules of alginate blocks. The TEP formation was the result of the intermolecular interactions between these blocks. Accordingly, in this study we deduced that TEPs possessed large sizes and easily attached on a membrane surface to form a fouling layer which in turn prevented the serious pore clogging of the membrane. In addition, the TEP level indicated the extent of intermolecular interactions of polysaccharides, which was an important factor influencing membrane fouling.

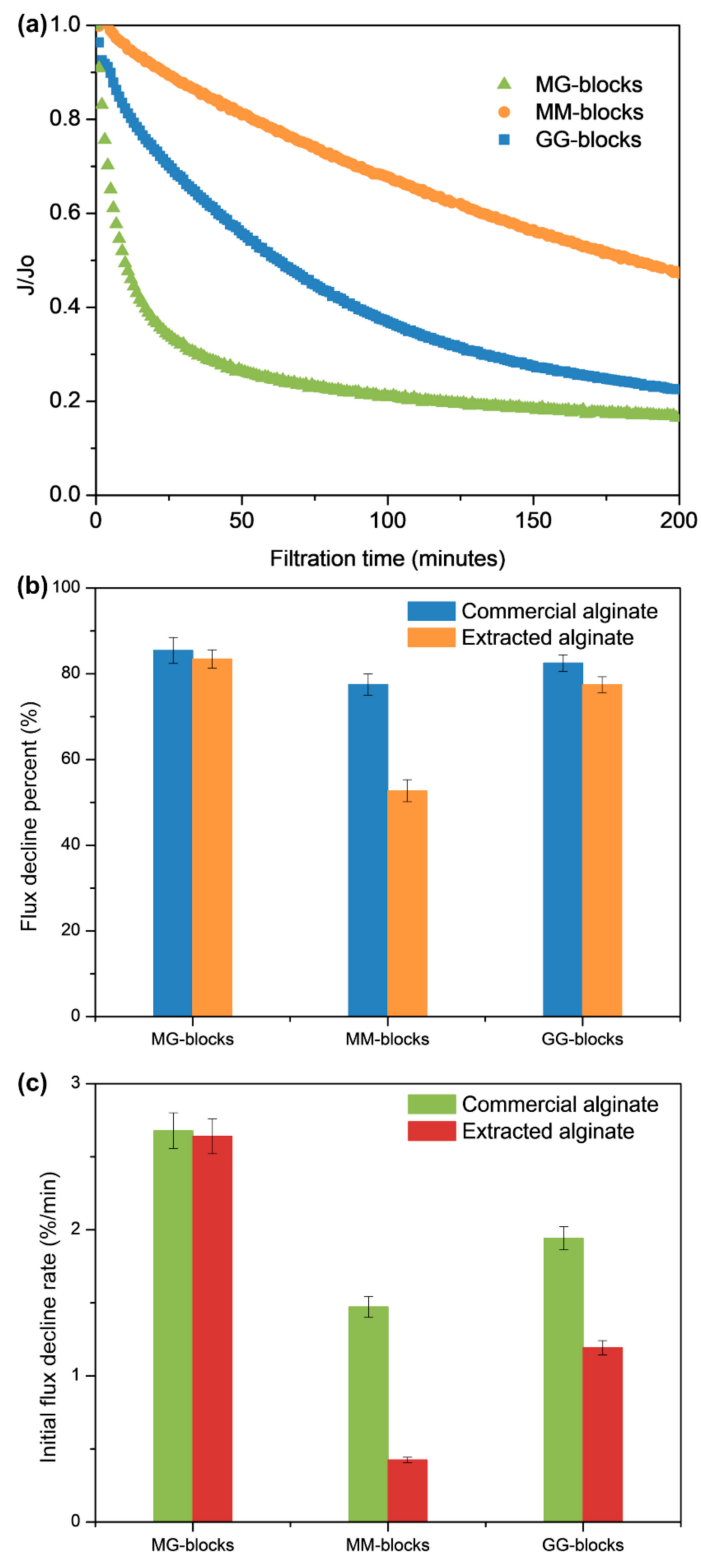


**Figure 7.** (a) Flux profiles of MG-, MM- and GG-blocks at 50 mg/L; (b) the final flux decline percentage and the (c) initial flux decline rates of alginate blocks derived from commercial and extracted alginates.

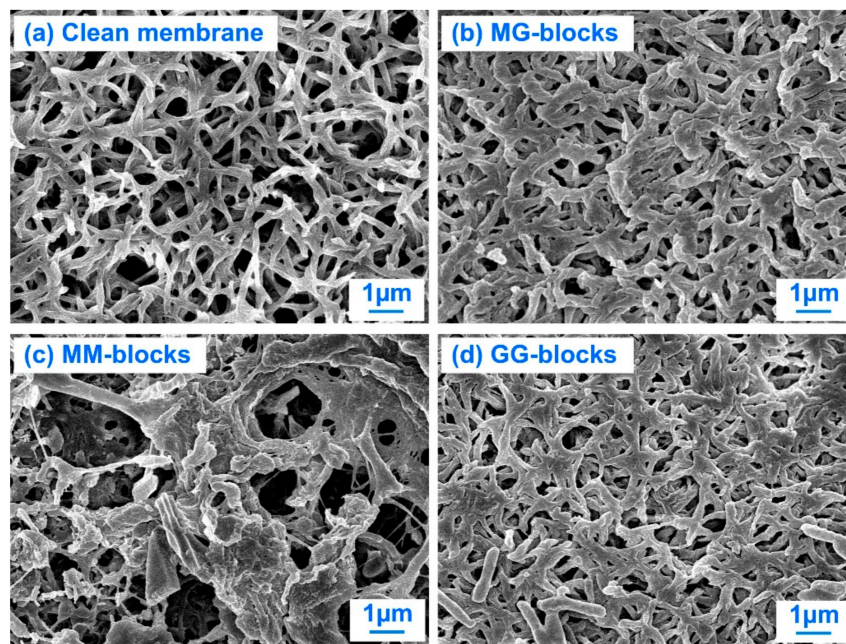


**Figure 8.** FESEM observations of the (a) clean membrane and membrane surfaces fouled by (b) MG-, (c) MM- and (d) GG-blocks.

It appears that this conclusion is different from the general understanding of TEPs—that they accelerate the membrane fouling [31–33]. However, it should be noted that the role of TEPs in membrane fouling is not a black and white issue. TEPs are easy to attach onto a membrane surface and promote fouling layer formation on a membrane. For the non-porous membrane and the membrane with small pores, TEPs may promote fouling layer development during membrane filtration which contributes to the filtration resistance. Differently, it turned out that the fouling layer acted as pre-filter to prevent the serious pore blocking of membranes in this study, which on the contrary, did not lead to serious fouling problems. Consequently, the TEP fouling is a complicated issue which also depends on the characteristics of membrane and the operation conditions and so on. Nevertheless, with high viscosity and big size, TEPs are prone to attach onto membranes compared to other foulants. More importantly, the TEP formation indicates the potential of polysaccharide crosslinking, which is an important issue in membrane fouling. These findings reveal that the molecular chains of polysaccharides do not exist singly, by themselves in a free state, but they usually combine together to form big three dimensional networks. The crosslinking abilities of polysaccharides vary from one to another dramatically, which in turn affects their fouling propensities. Combined with the results obtained in this study, it can be concluded that polysaccharides with different molecular compositions would have different characteristics, including their effects on membrane fouling. Therefore, future studies should pay attention to the molecule structures of foulant and the crosslinking between foulant molecules.

#### 4. Conclusions

Alginate is abundant in natural water environments and consists of three different blocks; i.e., MG-, MM- and GG-blocks. In this study, an alginate sample was first extracted from the raw seaweed and then well characterized with fractionation, FTIR and FESEM. Results confirmed the existence of alginate in the seaweed and showed that the main component in this alginate was the MM-blocks. FTIR spectra of extracted MG-, MM- and GG-blocks illustrated a similar chemical composition with commercial alginate blocks. What is more important, is that the TEP measurement showed that MG-, MM- and GG-blocks possessed different abilities in forming TEP via molecular crosslinking. Furthermore, the filtration tests of the three kinds of alginate blocks demonstrated totally different flux

profiles, indicating that they do have diverse fouling propensities. So far, many studies have employed alginate as a model foulant. However, our results reveal that alginates with different molecular compositions behave differently in membrane filtration experiments. It is a reasonable consideration that future work should include analysis of the alginate in question's molecular composition in order to obtain more reliable results.

**Author Contributions:** S.M. and L.W. conceived and designed the experiments; R.W. and S.M. performed the experiments; R.W. and X.M. analyzed the data; H.L. and M.Z. contributed reagents/materials/analysis tools; S.M. and L.W. wrote the paper.

**Acknowledgments:** This work was financially supported by grants from the National Natural Science Foundation of China (number 51808019) and this research received no external funding.

**Conflicts of Interest:** The authors declare no conflict of interest.

## References

1. Qu, C.; Lu, S.; Liang, D.; Chen, S.; Xiang, Y.; Zhang, S. Simultaneous electro-oxidation and in situ electro-peroxone process for the degradation of refractory organics in wastewater. *J. Hazard. Mater.* **2019**, *364*, 468–474. [[CrossRef](#)] [[PubMed](#)]
2. Liu, S.; Cui, M.; Li, X.; Thuyet, D.Q.; Fan, W. Effects of hydrophobicity of titanium dioxide nanoparticles and exposure scenarios on copper uptake and toxicity in *Daphnia magna*. *Water Res.* **2019**, *154*, 162–170. [[CrossRef](#)] [[PubMed](#)]
3. Hu, R.; Gwenzi, W.; Sipowo-Tala, V.R.; Noubactep, C. Water Treatment Using Metallic Iron: A Tutorial Review. *Processes* **2019**, *7*, 622. [[CrossRef](#)]
4. Qu, C.; Soomro, G.S.; Ren, N.; Liang, D.-W.; Lu, S.-F.; Xiang, Y.; Zhang, S.-J. Enhanced electro-oxidation/peroxone (in situ) process with a Ti-based nickel-antimony doped tin oxide anode for phenol degradation. *J. Hazard. Mater.* **2019**, 121398. [[CrossRef](#)] [[PubMed](#)]
5. Elimelech, M.; Phillip, W.A. The Future of Seawater Desalination: Energy, Technology, and the Environment. *Science* **2011**, *333*, 712–717. [[CrossRef](#)]
6. Zamora, S.; Sandoval, L.; Marín-Muñoz, J.L.; Fernández-Lambert, G.; Hernández-Orduña, M.G. Impact of Ornamental Vegetation Type and Different Substrate Layers on Pollutant Removal in Constructed Wetland Mesocosms Treating Rural Community Wastewater. *Processes* **2019**, *7*, 531. [[CrossRef](#)]
7. Bis, M.; Montusiewicz, A.; Piotrowicz, A.; Łagód, G. Modeling of Wastewater Treatment Processes in Membrane Bioreactors Compared to Conventional Activated Sludge Systems. *Processes* **2019**, *7*, 285. [[CrossRef](#)]
8. Song, Y.; Motuzas, J.; Wang, D.K.; Birkett, G.; Smart, S.; Diniz da Costa, J.C. Substrate Effect on Carbon/Ceramic Mixed Matrix Membrane Prepared by a Vacuum-Assisted Method for Desalination. *Processes* **2018**, *6*, 47. [[CrossRef](#)]
9. Wagh, P.; Zhang, X.; Blood, R.; Kekenés-Huskey, P.M.; Rajapaksha, P.; Wei, Y.; Escobar, I.C. Increasing Salt Rejection of Polybenzimidazole Nanofiltration Membranes via the Addition of Immobilized and Aligned Aquaporins. *Processes* **2019**, *7*, 76. [[CrossRef](#)]
10. Martin Vincent, N.; Tong, J.; Yu, D.; Zhang, J.; Wei, Y. Membrane Fouling Characteristics of a Side-Stream Tubular Anaerobic Membrane Bioreactor (AnMBR) Treating Domestic Wastewater. *Processes* **2018**, *6*, 50. [[CrossRef](#)]
11. Berman, T.; Holenberg, M. Don't fall foul of biofilm through high TEP levels. *Filtr. Sep.* **2005**, *42*, 30–32. [[CrossRef](#)]
12. Passow, U. Transparent exopolymer particles (TEP) in aquatic environments. *Prog. Oceanogr.* **2002**, *55*, 287–333. [[CrossRef](#)]
13. Wang, R.; Liang, D.; Liu, X.; Fan, W.; Meng, S.; Cai, W. Effect of magnesium ion on polysaccharide fouling. *Chem. Eng. J.* **2020**, 379. [[CrossRef](#)]
14. Bar-Zeev, E.; Passow, U.; Castrillon, S.R.; Elimelech, M. Transparent exopolymer particles: From aquatic environments and engineered systems to membrane biofouling. *Environ. Sci. Technol.* **2015**, *49*, 691–707. [[CrossRef](#)] [[PubMed](#)]

15. Draget, K.I.; Smidsrød, O.; Skjåk-Bræk, G. Alginates from Algae. In *Biopolymers Online*; Wiley-VCH Verlag GmbH & Co. KGaA: Weinheim, Germany, 2005. [[CrossRef](#)]
16. Melvik, J.; Dornish, M. Alginate as a Carrier for Cell Immobilisation. In *Fundamentals of Cell Immobilisation Biotechnology*; Nedović, V., Willaert, R., Eds.; Springer: Amsterdam, The Netherlands, 2004; Volume 8A, pp. 33–51.
17. Tønnesen, H.H.; Karlsen, J. Alginate in Drug Delivery Systems. *Drug Dev. Ind. Pharm.* **2002**, *28*, 621–630. [[CrossRef](#)] [[PubMed](#)]
18. Lee, K.Y.; Mooney, D.J. Alginate: Properties and biomedical applications. *Prog. Polym. Sci.* **2012**, *37*, 106–126. [[CrossRef](#)] [[PubMed](#)]
19. Leal, D.; Matsuhira, B.; Rossi, M.; Caruso, F. FT-IR spectra of alginic acid block fractions in three species of brown seaweeds. *Carbohydr. Res.* **2008**, *343*, 308–316. [[CrossRef](#)]
20. Meng, S.; Liu, Y. New insights into transparent exopolymer particles (TEP) formation from precursor materials at various Na<sup>+</sup>/Ca<sup>2+</sup> ratios. *Sci. Rep.* **2016**, *6*, 19747. [[CrossRef](#)]
21. Meng, S.; Winters, H.; Liu, Y. Ultrafiltration behaviors of alginate blocks at various calcium concentrations. *Water Res.* **2015**, *83*, 248–257. [[CrossRef](#)]
22. Chandía, N.P.; Matsuhira, B.; Mejías, E.; Moenne, A. Alginic acids in *Lessonia vadosa*: Partial hydrolysis and elicitor properties of the polymannuronic acid fraction. *J. Appl. Phycol.* **2004**, *16*, 127–133. [[CrossRef](#)]
23. Steyermark, A. *Spectrometric Identification of Organic Compounds*, 3rd ed.; Silverstein, R.M., Bassler, G.C., Morrill, T.C., Eds.; Wiley: New York, NY, USA, 1974; p. 340. [[CrossRef](#)]
24. Mathlouthi, M.; Koenig, J.L. Vibrational Spectra of Carbohydrates. In *Advances in Carbohydrate Chemistry and Biochemistry*; Tipson, R.S., Derek, H., Eds.; Academic Press: Cambridge, MA, USA, 1987; Volume 44, pp. 7–89.
25. Gómez-Ordóñez, E.; Rupérez, P. FTIR-ATR spectroscopy as a tool for polysaccharide identification in edible brown and red seaweeds. *Food Hydrocoll.* **2011**, *25*, 1514–1520. [[CrossRef](#)]
26. Coimbra, M.A.; Barros, A.; Barros, M.; Rutledge, D.N.; Delgadillo, I. Multivariate analysis of uronic acid and neutral sugars in whole pectic samples by FT-IR spectroscopy. *Carbohydr. Polym.* **1998**, *37*, 241–248. [[CrossRef](#)]
27. Synytsya, A.; Kim, W.-J.; Kim, S.-M.; Pohl, R.; Synytsya, A.; Kvasnička, F.; Čopíková, J.; Il Park, Y. Structure and antitumour activity of fucoidan isolated from sporophyll of Korean brown seaweed *Undaria pinnatifida*. *Carbohydr. Polym.* **2010**, *81*, 41–48. [[CrossRef](#)]
28. Meng, S.; Liu, Y. Alginate block fractions and their effects on membrane fouling. *Water Res.* **2013**, *47*, 6618–6627. [[CrossRef](#)] [[PubMed](#)]
29. Meng, S.; Fan, W.; Li, X.; Liu, Y.; Liang, D.; Liu, X. Intermolecular interactions of polysaccharides in membrane fouling during microfiltration. *Water Res.* **2018**, *143*, 38–46. [[CrossRef](#)]
30. Wang, X.; Fan, W.; Dong, Z.; Liang, D.; Zhou, T. Interactions of natural organic matter on the surface of PVP-capped silver nanoparticle under different aqueous environment. *Water Res.* **2018**, *138*, 224–233. [[CrossRef](#)]
31. Berman, T.; Mizrahi, R.; Dosoretz, C.G. Transparent exopolymer particles (TEP): A critical factor in aquatic biofilm initiation and fouling on filtration membranes. *Desalination* **2011**, *276*, 184–190. [[CrossRef](#)]
32. Villacorte, L.O.; Kennedy, M.D.; Amy, G.L.; Schippers, J.C. Measuring transparent exopolymer particles (TEP) as indicator of the (bio)fouling potential of RO feed water. *Desalin. Water Treat.* **2009**, *5*, 207–212. [[CrossRef](#)]
33. Bar-Zeev, E.; Berman-Frank, I.; Liberman, B.; Rahav, E.; Passow, U.; Berman, T. Transparent exopolymer particles: Potential agents for organic fouling and biofilm formation in desalination and water treatment plants. *Desalin. Water Treat.* **2009**, *3*, 136–142. [[CrossRef](#)]

